



Springer

Dear Author:

Please find attached the final pdf file of your contribution, which can be viewed using the Acrobat Reader, version 3.0 or higher. We would kindly like to draw your attention to the fact that copyright law is also valid for electronic products. This means especially that:

- You may not alter the pdf file, as changes to the published contribution are prohibited by copyright law.
- You may print the file and distribute it amongst your colleagues in the scientific community for scientific and/or personal use.
- You may make an article published by Springer-Verlag available on your personal home page provided the source of the published article is cited and Springer-Verlag is mentioned as copyright holder. You are requested to create a link to the published article in LINK, Springer's internet service. The link must be accompanied by the following text: The original publication is available on LINK **<http://link.springer.de>**. Please use the appropriate URL and/or DOI for the article in LINK. Articles disseminated via LINK are indexed, abstracted and referenced by many abstracting and information services, bibliographic networks, subscription agencies, library networks and consortia.
- You are not allowed to make the pdf file accessible to the general public, e.g. your institute/your company is not allowed to place this file on its homepage.
- Please address any queries to the production editor of the journal in question, giving your name, the journal title, volume and first page number.

Yours sincerely,

Springer-Verlag Berlin Heidelberg

S. Constable · A. Duba

## Diffusion and mobility of electrically conducting defects in olivine

Received: 18 October 2000 / Accepted: 7 May 2002

**Abstract** Electrical conductivity of lherzolite (65% olivine), measured as a function of time after changes in the oxygen fugacity ( $f_{O_2}$ ) of the surrounding  $CO_2/CO$  atmosphere, is used to infer the diffusivity of the point defects responsible for conduction in olivine. A total of 63 equilibration runs at temperatures of 900, 1000, 1100, and 1200 °C were fit using nonlinear parameter estimation to recover time constants (directly related to diffusivity) and conductivity steps. An observed  $f_{O_2}$  dependence in the time constants associated with re-equilibration implies two defect species of fixed diffusivity but with  $f_{O_2}$ -dependent concentrations. Although the rate-limiting step may not necessarily be associated with a conducting defect, when time constants are converted to diffusivities, the magnitudes and activation energies agree extremely well with the model for magnesium vacancies (the slower species) and small polarons (holes localized on  $Fe^{3+}$ ) derived by Constable and Roberts (1997). This earlier study used an independent method of simultaneous modeling of thermopower and electrical conductivity as a function of  $f_{O_2}$  and temperature, on data from a different type of sample (a dunite). We observe that at high  $f_{O_2}$  where polarons dominate over magnesium vacancies in the defect population, re-equilibration is dominated by magnesium vacancy diffusion, and vice versa (at low  $f_{O_2}$  magnesium vacancies dominate and re-equilibration proceeds at the faster rate associated with polaron mobility). We interpret this to suggest association between the cation vacancies and polarons, as has been suggested by Tsai and Dieckmann

(1997), making the concentration of the minority defect the rate-limiting step in the oxidation/reduction reactions.

**Keywords** Defect chemistry · Electrical conductivity · Olivine

### Introduction

Defect chemistry is important in the study of the electrical conductivity of Earth's mantle. Currently, it is difficult to make measurements of the electrical conductivity of mantle materials under simultaneously controlled conditions of pressure, temperature, oxygen fugacity, water activity, silica activity, and iron activity. A thorough understanding of the point-defect mechanisms that determine conductivity in olivine-rich rocks will help us extrapolate laboratory measurements to conditions applicable to the mantle. In addition, this understanding can be used as a guide to the effect of these parameters on the conductivity of high-pressure mineral phases in the mantle.

Because silicates are insulators or, at best, poor semiconductors, their electrical conductivity  $\sigma$  depends strongly on the defect population, and because electrical measurements are relatively straightforward, the effects of variation of environmental parameters on defect population can be monitored easily and with high accuracy. In the apparatus used for this study (Duba et al. 1990), conductivity can be determined within an error of 0.2 of a log unit, temperature within 3 K, and oxygen fugacity within 0.1 of a log unit. In each case, the precision of the measurement during a single sample run is much higher than the stated accuracy.

For a material in which  $\sigma$  depends on oxygen fugacity  $f_{O_2}$ , under favorable circumstances the variation of  $\sigma$  resulting from changes in  $f_{O_2}$ , at constant temperature, can be used to infer diffusion of defects associated with re-equilibration (e.g., Franke and Dieckmann 1987). Olivine  $\sigma$  depends on  $f_{O_2}$ , and Schock et al. (1989) noted that at 1200 °C conductivity changes came to

S. Constable (✉)  
Institute of Geophysics and Planetary Physics,  
Scripps Institution of Oceanography,  
La Jolla California 92093-0225, USA  
e-mail: sconstable@ucsd.edu

A. Duba  
Earth and Planetary Sciences Department,  
American Museum of Natural History,  
Central Park West at 79th St,  
NYC New York 10024-5192, USA

“equilibrium” values in less than 1 h after changes of the gas mixture that controlled  $f_{O_2}$ . While measuring the conductivity of the Mount Porndon lherzolite (65% olivine) as a function of  $f_{O_2}$ , Duba and Constable (1993) studied conductivity changes associated with changes in gas mixture. They obtained data that were consistent with diffusion data reported in a study by Mackwell et al. (1988) of relaxation data in olivine creep experiments. Because Mackwell et al. analyzed their creep relaxation data in terms of magnesium vacancies, while the conducting species in olivine is inferred to be the small polaron (Schock et al. 1989), Duba and Constable (1993) argued that the production of polarons resulting from oxidation of iron depends on the creation of magnesium vacancies as the rate-limiting step. A similar study was undertaken by Wanamaker (1994), who also inferred magnesium vacancy diffusion but fit a second, faster, time constant to olivine single-crystal data and associated it with silicon vacancies ( $V_{Si}^{m}$ ).

The present paper is an attempt to improve the preliminary investigations of Duba and Constable (1993) and Wanamaker (1994) by extending the temperature range of the previous studies; making the gas change that is responsible for the  $f_{O_2}$  change more step-like; and effecting improvements in the modeling algorithms. It is our intent to demonstrate that the application of carefully controlled electrical conductivity measurements provides extra insight into physical processes pertinent to diffusion, electrical conductivity, and creep experiments in mantle materials.

## Experimental

The sample used in this study is a lherzolite from Mt. Porndon, Australia, with approximate modal composition 3% clinopyroxene, 31% orthopyroxene, 1% spinel, and 65% olivine (M. Drury, personal communication, 1992), with a grain size of approximately 1 mm. Although porosity was not measured, optical examination found only small amounts of crack porosity in the clean, unaltered sample selected for conductivity measurement. In addition, grain boundaries appeared sharp and unaltered, and we estimate porosity at less than 1%. Sample preparation and electrical conductivity measurements were carried out using the two-electrode method as described in detail by Duba et al. (1990), and summarized here. The sample was a disk 7.0 mm in diameter and 1.3 mm thick, and polished on the flat electrode surfaces to a 4-micron finish. This sample geometry is determined by the apparatus, the low electrical conductivity of olivine (requiring a thin sample), and the fabric of the rock. In order to inhibit iron loss to the circular electrodes, a pair of 0.05-mm-thick iridium foils isolate the sample from the 0.25-mm-thick Pt foil to which Pt/Pt 10% Rh thermocouples are welded. Electrical conductivity was measured with an automated impedance bridge operating at frequencies of 0.1, 1.0, and 10 kHz. Although complex impedance depends on frequency, the bridge estimates the magnitude of the resistance at any given frequency, which provides an accurate estimate of conductivity as long as one operates at frequencies in the grain-interior regime, which we do (see the discussion in Duba and Constable 1993).

Oxygen fugacity,  $f_{O_2}$ , was controlled using a mixture of CO and CO<sub>2</sub> at total pressure of 1 atm (Deines et al. 1974) with no dilution, flowing by the sample in a furnace with a positive upstream pressure of 50 kPa and vented into the exhaust of a fume hood on the downstream side. Conductivity was measured as a function of time

as oxygen fugacity was changed at constant temperatures of 900, 1000, 1100, and 1200 °C. The change of gas mixture was made as step-like as possible by changing the gas mixture quickly and by making no adjustments between changes, a practice not followed in previous studies, where we were more concerned about attaining target  $f_{O_2}$  values by adjusting the mixture during the first 10 to 15 min following the initial gas change. This modification required only 0.2 to 0.5 min to dial in the desired gas mixture on the mass-flow controllers during a gas change. The result was a dramatic improvement in the form of the conductivity variation with time so that fits to the data are more accurate. Experimental  $f_{O_2}$  is measured in a calcia-doped zirconia cell maintained at a temperature of 1200 °C, and so  $f_{O_2}$  at the sample temperature  $T$  is computed using Eq. (14) from Constable and Roberts (1997):

$$\log_{10}(f_{O_2})_T = \log_{10}(f_{O_2})_{1200^\circ C} + 29530 \left( \frac{1}{1473} - \frac{1}{T} \right),$$

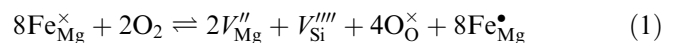
where  $T$  is in Kelvin.

By choosing to work with a rock, rather than a single crystal or synthetic compact, we lose some control of grain size and composition. However, since our sample, Mt. Porndon lherzolite, is a mantle-derived material (Irving 1980), we are more likely to be dealing with physical and chemical processes appropriate to conduction within the mantle, and in particular the chemical buffering environment is complete and appropriate to the mantle. The latter is important;  $\sigma(f_{O_2})$  behavior is observed to be dependent on silica buffering in olivine (Wanamaker and Duba 1993). Because olivine makes up more than 60% of the lherzolite, olivine conductivity will predominate unless there is an interconnected grain-boundary phase. In addition, the electrical conductivity of orthopyroxene is slightly less than that of olivine for a given iron content and has a similar dependence on oxygen fugacity (Duba et al. 1973).

Although one might expect that intergranular faces in a polycrystalline sample are forced open by temperature, there is no evidence of this in the electrical conductivity data (Duba and Constable 1993), and examination of other polycrystals using TEM shows that the faces can be closed in some circumstances (J.J. Roberts, personal communication). When removed from the furnace, our samples are typically intact and competent. Small traces of hydrous phases are undoubtedly present in natural samples, but we seek unaltered material, and assume that any hydrous material present decomposes rapidly upon initial heating.

## Dependence of electrical conductivity on oxygen fugacity

At the heart of our ability to use electrical conductivity to study point-defect relaxation is the  $f_{O_2}$  dependence that conductivity exhibits. If conduction in olivine is by means of polarons localized on  $Fe_{Mg}^\bullet$  then the relationship between conduction and  $f_{O_2}$  has been described by



(Smyth and Stocker 1975; Schock et al. 1989). This model predicts that  $\sigma$  will have a dependence on  $f_{O_2}$  of the form

$$\sigma = \sigma_o(f_{O_2})^{1/6} \quad (2)$$

However, measurements of  $\sigma(f_{O_2})$  in pyroxene-buffered olivines generally have slopes much smaller than 1/6, which decrease even further at low  $f_{O_2}$ , and we have speculated as to why this might be (e.g., Constable and Duba 1990; Duba and Constable 1993; Constable and Roberts 1997). Although our understanding of the point-defect chemistry in olivine is thus clearly incomplete, the observation that conductivity is a function of

**Fig. 1** Conductivity as a function of  $f_{O_2}$  at the various temperatures used in this study: triangles 900 °C; octagons 1000 °C; diamonds 1100 °C; pluses 1200 °C

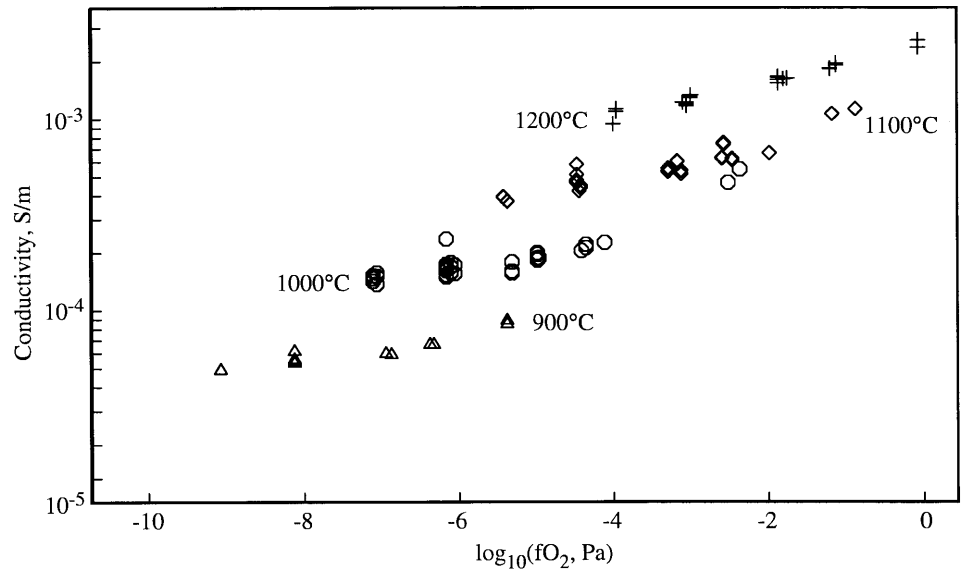


**Table 1** Linear fits to the  $\sigma$ - $f_{O_2}$  data of Fig. 1

Temp (°C)	Slope of $\log(\sigma)$ - $\log(f_{O_2})$	Slope <sup>-1</sup>
1200	0.0938 ± 0.0078	10.7
1100	0.0764 ± 0.0078	13.1
1000	0.0543 ± 0.0076	18.4
900	0.0603 ± 0.0096	16.6

$f_{O_2}$  change allows us to proceed with the re-equilibration measurements.

Our  $\sigma(f_{O_2})$  data for the current sample are shown in Fig. 1. These results agree very well with data collected on a similar sample at 1200 °C by Duba and Constable (1993), with the conductivities at  $10^{-3}$  Pa differing only by 10%. The data are, by and large, well fit by straight lines in log-log space (Table 1), that is a power law with a single term, although there is consistently the slight curvature seen in other studies and modeled by Duba and Constable (1993) and Constable and Roberts (1997) as a two-term power law. Although the slope of the  $\sigma(f_{O_2})$  relationship is small, about 1/11 at high temperature/high  $f_{O_2}$  and less at low temperature/low  $f_{O_2}$ , this signal is well within the precision of the conductivity apparatus.

We are also concerned about avoiding  $f_{O_2}$  conditions close to the edges of the olivine stability field in order to minimize irreversible changes in sample conductivity (Wanamaker and Duba 1993). We succeed in maintaining an almost constant conductivity (at given temperature and  $f_{O_2}$ ) throughout the experiment at the expense of collecting data at extreme  $f_{O_2}$  conditions. Over the 5000 h between the end of initial equilibration and the end of the experiment, conductivity at 1000 °C increased only 3% at the reference  $f_{O_2}$ . We attribute this slight increase in conductivity to a better contact between sample and electrode as a result of long anneals at high temperature.

Figure 2 is an example of the response of the electrical conductivity of lherzolite to a change in oxygen fugacity at 1000 °C. The circles in this particular

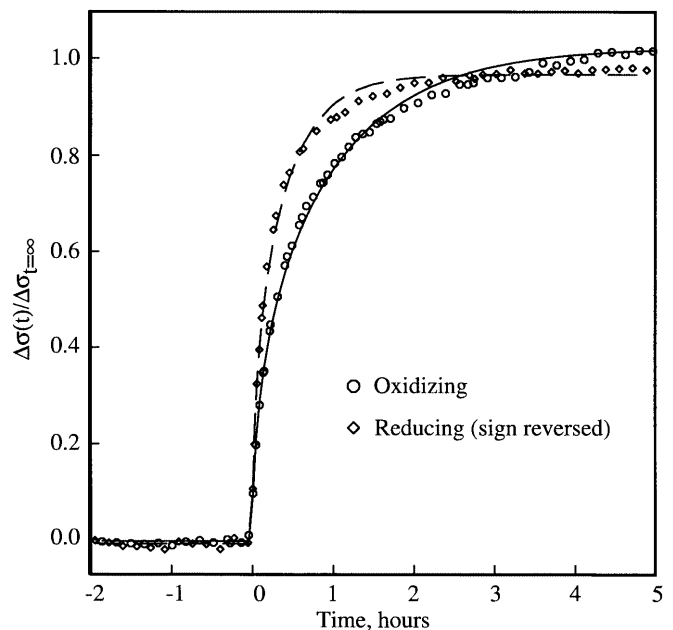


**Fig. 2** Normalized electrical conductivity at 1000 °C after step-function changes in  $f_{O_2}$  from  $10^{-6.2}$  Pa to  $10^{-5.0}$  Pa (Oxidizing) and  $10^{-5.0}$  Pa to  $10^{-6.2}$  Pa (Reducing). The sign of the reducing run has been reversed to make the shorter time constant for the reduction run evident. Lines through both data sets are model fits for diffusion in a sphere, as described in the text. The initial conductivity is about  $1.6 \times 10^{-4} \text{ Sm}^{-1}$ , and the conductivity change represents about a 12% change over this value. A slight hysteresis prevents the reducing run from completely reversing the effects of the oxidizing run, and so the two runs are not asymptotic to the same value

example are for the oxidation of a sample that is in equilibrium at an oxygen fugacity of  $10^{-6.2}$  Pa and oxidized to  $10^{-5.0}$  Pa. The diamonds are for the subsequent reduction of the material when it is in equilibrium at an oxygen fugacity of  $10^{-5.0}$  Pa to a new  $f_{O_2}$  of  $10^{-6.2}$  Pa. Note that the shapes of these exponentials are quite different and yield quite different time constants. (These data correspond to runs 441 and 450 in Table 2.)

**Table 2** Diffusivity data  $f_{O_2}$  values are quoted as  $\log_{10}(\text{Pa})$ 

Run ID	Temp (°C)	Starting $f_{O_2}$	Final $f_{O_2}$	$\tau$ , $10^3$ s	$\sigma_{\tau}$ , %
754	1200	-3.05	-1.80	3.60	2.3
762	1200	-1.75	-3.05	1.73	2.1
785	1200	-4.00	-3.05	2.48	1.6
805	1200	-3.05	-1.20	5.04	2.9
826	1200	-1.20	-3.05	2.09	3.0
834	1200	-3.10	-0.07	8.42	2.7
850	1200	-0.07	-3.05	2.81	2.5
3318	1200	-3.00	-3.96	2.52	17.9
3321	1200	-3.96	-3.00	2.41	18.9
3322	1200	-3.00	-1.87	4.50	16.7
3324	1200	-1.87	-1.12	7.99	12.1
3327	1200	-1.12	-1.87	11.12	8.0
3328	1200	-1.87	-3.00	2.74	5.2
610	1100	-4.51	-3.21	9.18	2.3
617	1100	-3.21	-4.51	4.50	2.6
634	1100	-4.51	-5.46	3.38	4.3
642	1100	-5.46	-4.51	9.14	3.5
658	1100	-4.51	-2.61	18.25	1.7
666	1100	-2.61	-4.51	4.21	2.8
682	1100	-4.51	-1.21	21.17	2.3
689	1100	-0.91	-4.51	4.61	1.7
3296	1100	-4.46	-5.41	5.83	5.5
3298	1100	-5.41	-4.46	7.24	4.4
3300	1100	-4.46	-3.33	8.68	14.3
3301	1100	-3.33	-2.63	14.83	20.3
3303	1100	-2.63	-3.33	8.82	48.8
3305	1100	-3.33	-4.46	6.91	10.3
3347	1100	-4.48	-3.16	11.20	52.6
3349	1100	-3.16	-2.50	27.54	24.9
3350	1100	-2.50	-2.02	23.83	25.0
148	1000	-6.20	-5.35	24.08	3.9
236	1000	-5.35	-6.20	12.60	3.3
281	1000	-6.20	-7.15	8.39	4.7
300	1000	-7.15	-6.20	16.13	3.0
343	1000	-6.20	-5.35	29.52	2.6
418	1000	-5.35	-6.20	13.93	2.6
441	1000	-6.20	-5.00	33.05	2.0
450	1000	-5.00	-6.20	13.64	2.5
466	1000	-6.20	-7.15	8.46	3.0
473	1000	-7.15	-6.20	14.76	2.8
490	1000	-6.20	-4.45	40.36	5.2
498	1000	-4.45	-6.20	12.31	2.3
513	1000	-6.20	-2.40	178.88	20.9
522	1000	-2.55	-6.20	11.16	3.6
3245	1000	-6.09	-7.10	15.88	9.9
3254	1000	-7.10	-6.14	33.19	14.0
3260	1000	-6.14	-5.02	36.14	8.0
3268	1000	-5.02	-4.39	25.49	68.1
3272	1000	-4.39	-5.02	113.15	37.5
3274	1000	-5.02	-6.14	12.31	27.8
4454	1000	-6.09	-7.10	24.48	2.1
4531	1000	-7.10	-6.14	36.61	2.1
4640	1000	-6.14	-5.02	68.44	2.6
5313	1000	-6.09	-7.10	26.10	1.8
5415	1000	-7.10	-6.14	44.03	1.6
922	900	-8.19	-6.94	86.72	5.0
946	900	-7.01	-8.19	115.13	2.8
971	900	-8.19	-9.14	75.96	3.1
995	900	-9.14	-8.19	114.44	8.9
1089	900	-8.19	-6.44	316.51	5.4
1114	900	-6.39	-8.19	145.66	1.8
1311	900	-8.19	-5.44	720.22	13.5
1361	900	-5.44	-8.19	164.45	0.8

## Modeling defect diffusion

Crank (1975) provides expressions for the ratio of the total mass of diffused material at time  $t$  as a ratio of the total mass that diffuses over all time, or  $M_t/M_{\infty}$ , for a variety of geometries and boundary conditions. For a step function in concentration at the surface of the sample at time  $t_0$ , the expressions for a sphere, cylinder and sheet can all be rewritten in the form

$$\frac{M_t}{M_{\infty}} = 1 - c_1 \sum_{i=1}^{\infty} \frac{1}{c_2(i)} e^{-c_2(t-t_0)/\tau}, \quad (3)$$

where the constants  $c_1$  and  $c_2$  take the following values for the different geometries:

$$\begin{array}{l} \text{Sphere} \\ \text{Cylinder} \\ \text{Sheet} \end{array} \left( \begin{array}{cc} c_1 & c_2(i) \\ 6 & \pi^2 i^2 \\ 4 & (j_{0,i})^2 \\ 2 & \pi^2 (i - 1/2)^2 \end{array} \right). \quad (4)$$

The  $j_{0,i}$  are the  $i$ th zeros of the Bessel function of the first kind and order zero, that is  $J_0(x) = 0$ , which we computed using a nonlinear optimization algorithm. The first 20 zeros can be found in Table 9.5 (p. 409) of Abramowitz and Stegun (1964). We have defined a time constant  $\tau$  equal to  $l^2/D$ , where  $D$  is diffusivity and  $l$  is the characteristic length of the sample (radius for sphere and cylinder, half-thickness for a sheet). If the average concentration of charge carriers is linearly proportional to the mass of diffused material, and if we assume that oxygen exchange at the sample/gas interface is much faster than chemical diffusion in the sample, then relative mass diffused is easily related to conductivity by

$$\sigma(t) = \sigma_i + \Delta\sigma \frac{M_t}{M_{\infty}}, \quad (5)$$

where  $\sigma_i$  is the initial conductivity before the change in  $f_{O_2}$  and  $\Delta\sigma$  is the change in conductivity caused by the  $f_{O_2}$  step, so

$$\sigma(t) = \sigma_i + \Delta\sigma \left( 1 - c_1 \sum_{i=1}^{\infty} \frac{1}{c_2} e^{-c_2(t-t_0)/\tau} \right). \quad (6)$$

Unfortunately, we cannot demonstrate a priori that the concentration of charge carriers depends linearly with the mass of the diffused species associated with the re-equilibration reaction. (Indeed, the details of the defect chemistry associated with the effect of  $f_{O_2}$  on olivine are still subject to debate.) A nonlinear dependence of conductivity on diffused mass would correspond to  $m \neq 1$  in the terminology of Franke and Dieckmann's (1987) Eq. (19). However, these authors report that significant variations in the value of  $m$  affect the results of re-equilibration kinetics only slightly. Furthermore, we will show that the rate-limiting defects associated with re-equilibration are probably the dominant charge carriers themselves, thereby assuring that  $m = 1$ .

The nonlinear equations given above are amenable to Marquardt inversion (Marquardt 1963) if the appropriate partial derivatives for  $\tau$ ,  $\sigma_0$ , and  $t_0$  are computed:

$$\frac{\partial \sigma}{\partial \tau} = -\Delta\sigma \frac{c_1(t-t_0)}{\tau^2} \sum_{i=1}^{\infty} e^{-c_2(t-t_0)/\tau} \quad (7)$$

$$\frac{\partial \sigma}{\partial \Delta\sigma} = 1 - c_1 \sum_{i=1}^{\infty} \frac{1}{c_2} e^{-c_2(t-t_0)/\tau} \quad (8)$$

$$\frac{\partial \sigma}{\partial t_0} = -\Delta\sigma \frac{c_1}{\tau} \sum_{i=1}^{\infty} e^{-c_2(t-t_0)/\tau}. \quad (9)$$

In practice it requires about four terms of the infinite sum to obtain 1% accuracy in Eq. (6) at short times, but about five terms to obtain

similar accuracy in the derivatives (Eqs. 7, 8, and 9). We use 40 terms in the analysis. The time constant is parameterized as  $\log(\tau)$  to force positivity. In this way we can fit our data to any of these three simple geometries. In practice, there are no great differences in the quality of the fits between the three different geometries. In Fig. 2 we use a spherical model which approximates the average grain geometry and fits the data slightly better (the solid and broken lines show the models for oxidation and reduction respectively). The RMS misfit for oxidation is 0.16% and reduction 0.20%, with the largest individual misfit being 0.45% (relative to the initial conductivity of  $1.6 \times 10^{-4} \text{ Sm}^{-1}$ ). Although these fits are statistically adequate, there are systematic patterns to the misfit which make it difficult to make quantitative judgements about which geometry is most appropriate. The theory above does not take into account the variation in grain size that we have in our sample, but modeling series and parallel conduction through grains of mixed size suggests that the larger grains, which dominate the total volume, determine the time constant.

The fits allow us to compute time constants associated with each re-equilibration run. In general, the oxidation runs exhibit longer time constants than the reduction runs, by at least a factor of 2 and up to 1 order of magnitude.

## Results

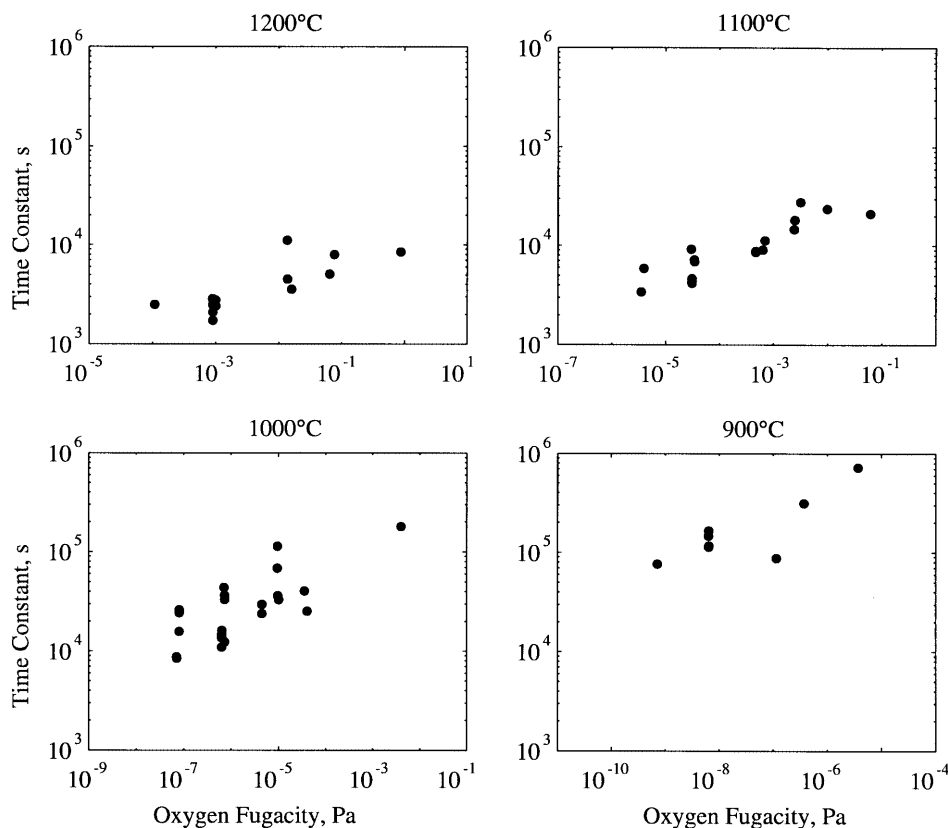
The observed asymmetry between oxidation and reduction suggests an  $f_{\text{O}_2}$ -dependent diffusion or similar phenomenon. To examine this, we fit each of the 64 runs using separate Marquardt inversions, solving for  $t_0$ ,  $\sigma_i$ ,  $\Delta\sigma$ , and  $\tau$  (initial time of  $f_{\text{O}_2}$  step, initial conductivity, conductivity step, and time constant) using the sphere model (Table 2). A total of 5800 h of data were collected at temperatures between 850 and 1200 °C, with 67

changes of gas mix. We discarded the four runs conducted at 850 °C as the low slope of  $\sigma(f_{\text{O}_2})$  and long re-equilibration times produced poor-quality data.

Our modeling of concentration-dependent diffusivity shows that the diffusivity associated with the final value of the gas mix dominates the behavior of re-equilibration (see also Crank 1975, p. 183). With this understanding, in Fig. 3 we plot the time constants as a function of final gas mix, to reveal a clear dependence of time constant on  $f_{\text{O}_2}$ . Some of the  $f_{\text{O}_2}$  steps are quite large, because we chose to return to a reference  $f_{\text{O}_2}$  after each change to monitor stability of the sample conductivity. (If the  $f_{\text{O}_2}$  dependence of  $\tau$  had been anticipated, we would have made much smaller steps in the gas mix, making the difference between initial and final  $f_{\text{O}_2}$  less important.)

Although these results could be interpreted in terms of concentration-dependent diffusivity of a single species, we have no reason to expect such a phenomenon at the low concentrations of the mobile defects in olivine (Hirsch and Shankland 1993). Rather, we will consider the hypothesis that the rate-limiting reaction is dominated by one species at low  $f_{\text{O}_2}$ , and a second species at higher  $f_{\text{O}_2}$ . To test this idea, we modified our code to include two diffusing species. We fit all the runs (data) at a given temperature simultaneously, allowing only two time constants,  $\tau_1$  and  $\tau_2$ , per temperature, but allowing the conductivity step associated with each run to vary. The conductivity step was divided into two parts,  $f_1$  and  $f_2$ , associated with the two time constants. That is,

**Fig. 3** Data in Table 2 plotted at the final value of  $f_{\text{O}_2}$  in the oxidation/reduction steps



$$\sigma(t) = \sigma_i + \Delta\sigma \left[ f_1 \left( 1 - c_1 \sum_{i=1}^{\infty} \frac{1}{c_2(i)} e^{-c_2(t-t_0)/\tau_1} \right) + f_2 \left( 1 - c_1 \sum_{i=1}^{\infty} \frac{1}{c_2(i)} e^{-c_2(t-t_0)/\tau_2} \right) \right]. \quad (10)$$

The parameters  $\sigma_i$  and  $t_0$  were fixed to be the values obtained from the single time constant fits to the individual runs and we solved only for  $(\Delta\sigma f_1)$  and  $(\Delta\sigma f_2)$ .

We are able to fit our data adequately this way, without significantly increasing the number of parameters (63 time constants and 63 conductivity steps are replaced by 8 time constants and 126 conductivity steps). The results fit our expectation of an  $f_{O_2}$ -dependent defect concentration. In Fig. 4 we plot the fraction of the re-equilibration attributed to the two mechanisms, and we see an almost monotonic dependence on (final)  $f_{O_2}$ .

Diffusivity,  $D$ , is calculated from the two time constants, evaluated at temperatures of 900, 1000, 1100, and 1200 °C, using

$$\tau = \frac{l^2}{D}$$

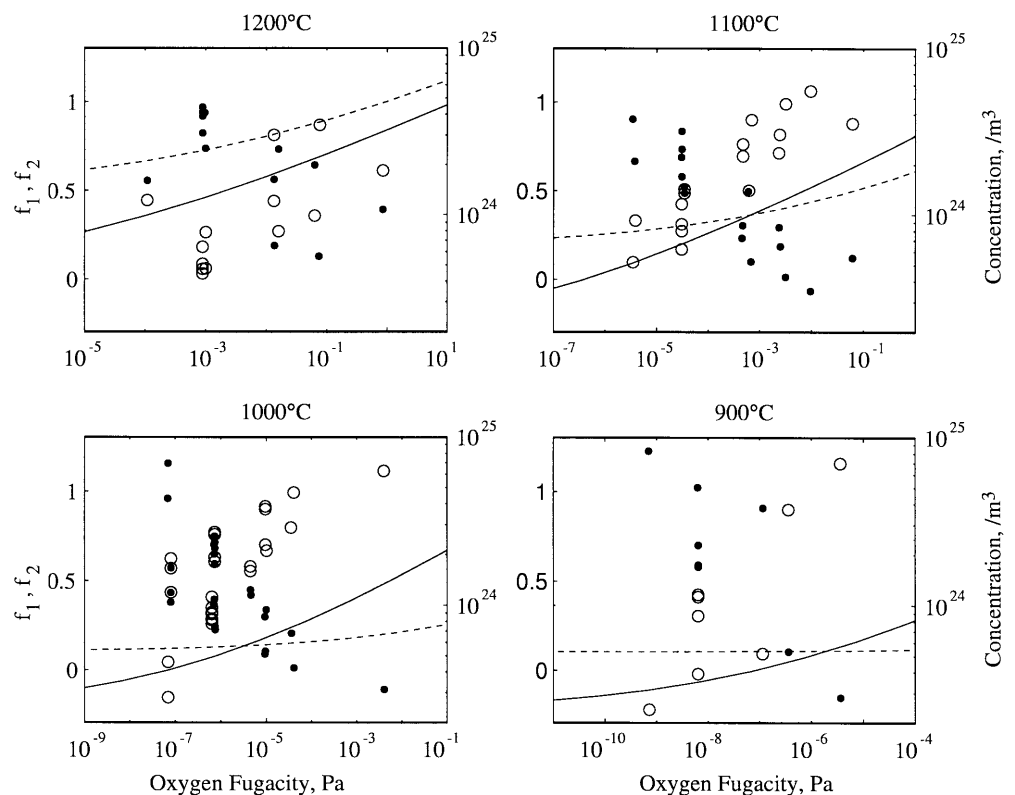
where  $l$  is the characteristic grain radius. Because the geometry and magnitude of our sample grain size are not well constrained,  $l^2$  is uncertain, and our diffusivity estimates could be systematically made larger or smaller by perhaps as much as half an order of magnitude. However, for  $l = 0.8$  mm our results agree extremely

well with diffusivities for polarons and magnesium vacancies computed from mobilities estimated by Constable and Roberts (1997), as shown in Fig. 5A. The agreement is indeed spectacular at temperatures between 1000 and 1200 °C, considering that Constable and Roberts' values are derived from a completely different methodology (simultaneous fitting of thermopower and conductivity as a function of  $f_{O_2}$  and temperature).

The agreement with the earlier work, in which the identity of the charge carriers was explicitly part of the modeling, yields the obvious conclusion that our two diffusivities are those of magnesium vacancies and polarons, and that the rate-limiting step for chemical re-equilibration in olivine is, in fact, determined by these two charged defects, the same defects responsible for electrical conduction over this temperature range. Because the rate-limiting defects appear to be the same as those that determine conductivity, our assumption that conductivity is linearly related to defect concentration is validated.

It is difficult to put error bounds on our results. Errors derived using linear statistics from the fitting are unrealistically small, and reflect the fact that the number of degrees of freedom in the problem is a lot less than the number of data. One may consider this also as covariance in the data, which may be seen in Fig. 2, where misfits tend to occur in groups of ten or so consecutive data points. Uncertainty in  $l$  does not affect the apparent activation energy, nor the ratio of diffusivities for the fast and slow species, both of which agree extremely well

**Fig. 4** Fractions  $f_1, f_2$  of conductivity step during re-equilibration attributed to the two different time constants, as a function of  $f_{O_2}$  and temperature. The fast time constant, inferred to be associated with  $Fe_{Mg}^\bullet$ , is shown as *small filled circles*, and the slow time constant, inferred to be  $V_{Mg}''$ , as *larger open circles*. Also shown is the concentration of  $Fe_{Mg}^\bullet$  (solid lines) and  $V_{Mg}''$  (broken lines) as computed from the model of Constable and Roberts (1997) (see right-hand scale)



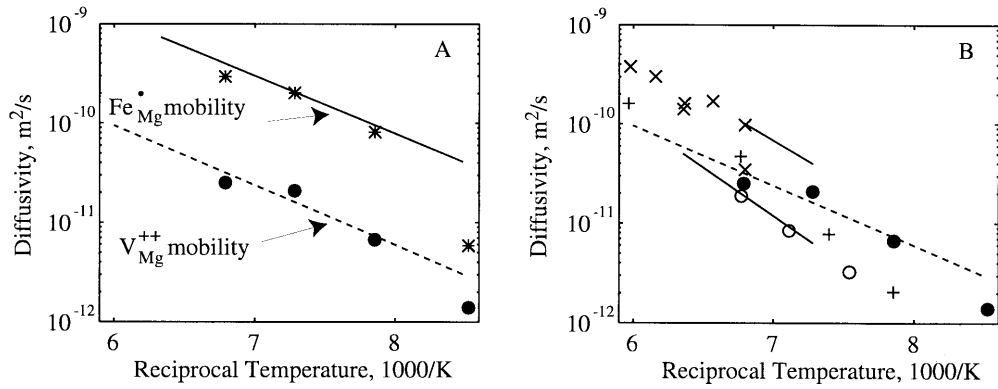


**Fig. 5** **A** Diffusivities derived from re-equilibration time constants when two conducting species are fit simultaneously (*filled circles and asterisks*) compared with diffusivities derived from mobilities of Constable and Roberts (1997) for polarons (*solid line*) and magnesium vacancies (*broken line*). Note that the lines are not fits to the new data, but represent independent work. **B** Diffusivities derived from re-equilibration time constants and inferred to be associated with magnesium vacancies (*filled circles*), and *broken line* compared with magnesium vacancy diffusivities from Wanamaker (1994) (*solid lines*), Mackwell et al. (1988) (*crosses*), Nakamura and Schmalzried (1984) (*open circles*), and Wanamaker (1986) (*pluses*)

with the thermopower/conductivity model, and so there seems little reason not to treat  $l$  as a free variable within reasonable limits (say within a factor of 2 of the sample thickness or estimated grain size), and use the Constable and Roberts results as a form of calibration for the experiment, as we did here. Similarly, uncertainty in the geometry associated with diffusion mathematics (sphere, cylinder, disk, range of grain sizes, etc.) has little effect on the results if the relationship between time constant and diffusivity is determined heuristically.

Our data at 900 °C do not fit the Constable and Roberts (1997) model quite so well. Re-equilibration at this temperature is slow, and the fitting appears to be dominated by the slower diffusivity – it appears very much as though the two time constants are both trying to fit the slower mechanism and are symmetric about the extrapolation of the  $V_{Mg}''$  mobility.

Figure 5B compares our results with other published estimates of magnesium vacancy diffusion (there are no measured mobilities for  $Fe_{Mg}^{\bullet}$  other than Constable and Roberts (1997)). The creep data of Mackwell et al. (1988) have a similar activation energy but with a magnitude that lies between our two mechanisms. It is tempting to infer that they observed a mixture of the two mechanisms. The Nakamura and Schmalzried (1984) data appear too low, and that study may indeed have been compromised by iron take-up by platinum during the experiment (Tsai and Dieckmann 1997). The Wanamaker (1994) results, derived in a way similar to ours using conductivity re-equilibration after  $f_{O_2}$  changes, show a similar ratio in magnitude and similar activation energies, but are systematically lower. This could easily be explained in terms of the effective dimension  $l$  used to convert time constants to diffusivities – the sample was approximated by an infinite thin sheet

in this case, and effects due to the finite aspect ratio and the electrodes were not included. The data of Wanamaker (1986), from re-equilibration of CO<sub>2</sub> inclusions, are of similar magnitude to our new data, although with slightly higher activation energy.

The agreement between the Constable and Roberts (1997) model and our present data suggests that further comparison should be made. Returning to Fig. 4, we have plotted the concentrations of  $Fe_{Mg}^{\bullet}$  and  $V_{Mg}''$  computed from the thermopower model. The concentrations of the two defects are similar, but with magnesium vacancies dominating at lower  $f_{O_2}$  and higher temperature. Note that because  $Fe_{Mg}^{\bullet}$  has a higher mobility, conductivity is inferred to be dominated by the polaron at all temperatures and  $f_{O_2}$  represented in this figure. We see a clear pattern in that when  $V_{Mg}''$  concentration exceeds  $Fe_{Mg}^{\bullet}$  concentration, re-equilibration is dominated by the diffusion of what we have inferred to be polarons. Similarly, when  $Fe_{Mg}^{\bullet}$  concentration exceeds  $V_{Mg}''$  concentration, equilibration is limited by an inferred magnesium vacancy mobility. This is similar to behavior seen in fayalite cation tracer diffusion by Tsai and Dieckmann (1997), who inferred that neutral associates form between cation vacancies and the polaron. Some association between  $V_{Mg}''$  and  $Fe_{Mg}^{\bullet}$  makes sense in terms of our current observations; the rate-limiting step for re-equilibration is determined by the minority defect.

## Discussion

Our observations are not unlike those made 26 years ago by Kitazawa and Coble (1974), who noted that diffusivity in Al<sub>2</sub>O<sub>3</sub> determined using electrical conductivity was lower for the oxidation runs and was higher the smaller the grain size. The polycrystalline manganosite sample of Keller and Dieckmann (1985) reported by Franke and Dieckmann (1987) had a similar asymmetry in conductivity re-equilibration, which these authors attributed to a rate-limiting surface reaction. In our case, a constant rate of oxygen adsorption would take longer at high  $f_{O_2}$  to satisfy the increased need for  $V_{Mg}''$ , and so we should consider the interaction of the sample with the experimental gas. It is unlikely that olivine

obtains oxygen from free oxygen gas in the experimental atmosphere; at 850 °C an  $f_{\text{O}_2, 1200^\circ\text{C}}$  of  $10^{-4}$  Pa corresponds to about  $10^{-15}$  atm of oxygen, or about 15 000 molecules  $\text{cm}^{-3}$  of gas. We assume rather that oxygen is taken from the  $\text{CO}_2$  in the gas mix. All the gas mixes used in this experiment have a  $\text{CO}_2/\text{CO}$  ratio of at least 10, so even though the oxygen partial pressure is changed over 4 orders of magnitude the  $\text{CO}_2$  pressure remains almost constant at 1 atm. Thus the need for oxygen increases much faster than the availability, and one might expect greater time constants at higher  $f_{\text{O}_2}$ , and see a slope of  $-1$ . However, reduction presents no such problem. The amount of CO in the experimental atmosphere increases a half order of magnitude for every order of magnitude decrease in  $f_{\text{O}_2}$ , and presumably oxygen can be lost through the formation of  $\text{O}_2$  on the surface of the sample. Although the reduction runs are systematically of higher diffusivity than the oxidation runs, this could be because the final values for the reduction runs are biased to lower  $f_{\text{O}_2}$ . There are enough reduction runs finishing at intermediate  $f_{\text{O}_2}$  to suggest a dependence on  $f_{\text{O}_2}$  similar to that observed for the oxidizing runs. Wanamaker (1994) used similar methodology on a single-crystal sample, yet reports no difference between oxidation and reduction. One would expect a rate-limiting surface reaction to be much more pronounced in a single crystal with a much smaller surface area-to-volume ratio than our sample. Finally, the results of Roberts and Duba (1995) indicate that the surface of olivine reacts relatively quickly to a change in gas mix. Thus, we conclude that the experimental atmosphere does not provide a rate-limiting step; this can be tested in future experiments by diluting the  $\text{CO}/\text{CO}_2$  mix with an inert gas, as has been done in similar studies on ceramics (including those of Franke and Dieckmann 1987 and Kitazawa and Coble 1974).

Wanamaker (1994) fit a second, faster, time constant nominated silicon vacancies ( $V_{\text{Si}}^{\text{Si}}$ ) to olivine single-crystal data on the basis that the longer time constant alone misfit the data at about the 5% level. The second term had a smaller contribution to the re-equilibration data, and the lower diffusivity/longer time constant dominates, although the misfit level was reduced. A faster diffusion mechanism associated with surface diffusion would be consistent with our own observations. With a small surface area-to-volume ratio, the effect of a fast diffusion mechanism operating on the surface of the single-crystal sample would have only a minor effect, while for the polycrystalline lherzolite it would be much greater. If the contribution from grain-boundary diffusion increased at low  $f_{\text{O}_2}$ , then most of what is observed could be explained, at least qualitatively. We note that the magnitude and  $f_{\text{O}_2}$  dependence of both conductivity and thermopower are almost identical for the single crystal and lherzolite (see Fig. 8 of Duba and Constable 1993 and Fig. 1, this paper), indicating strongly that, even though re-equilibration behavior is markedly different, the equilibrium conduction mechanism is basically the same.

## Conclusions

Monitoring equilibration of electrical conductivity after changes in the  $f_{\text{O}_2}$  of the sample environment is an effective way of estimating the diffusivity of species associated with defect chemistry in olivine. These may be the defects directly associated with conduction, or defects associated with a rate-limiting step in the electrochemical reaction that generates the conduction defects. Our analysis of 63 individual equilibrations at temperatures between 900 and 1200 °C exhibits an  $f_{\text{O}_2}$ -dependent diffusivity. We interpret these data in terms of two diffusing species having  $f_{\text{O}_2}$ -dependent concentrations, which is entirely consistent with other models of mixed conduction in olivine. Indeed, when an appropriate effective grain size is chosen, our diffusivities are almost identical to diffusivities calculated from  $\text{Fe}_{\text{Mg}}^\bullet$  and  $V_{\text{Mg}}''$  mobilities estimated by Constable and Roberts (1997). For the polaron, these diffusivities between 900 and 1200 °C are described in Constable and Roberts' model by

$$D_{\text{Fe}} = 3.78 \times 10^{-6} e^{-1.16\text{eV}/kT} \text{ m}^2 \text{ s}^{-1},$$

or, equivalently, an activation energy of  $1.86 \times 10^{-19}$  J. For the magnesium vacancy, the diffusivities between 900 and 1200 °C are described by

$$D_{\text{Mg}} = 4.21 \times 10^{-7} e^{-1.20\text{eV}/kT} \text{ m}^2 \text{ s}^{-1},$$

or, equivalently, an activation energy of  $1.92 \times 10^{-19}$  J. The agreement with the independently estimated mobilities for  $\text{Fe}_{\text{Mg}}^\bullet$  and  $V_{\text{Mg}}''$  removes any ambiguity concerning the nature of the diffusing species observed by our experiments, and, taken together, implies that these mobility/diffusivity estimates are very reliable.

The lack of a reported  $f_{\text{O}_2}$  dependence in single-crystal olivine equilibration studies suggests that a rate-limited surface reaction is not responsible for our observations in the polycrystal, but that a grain-boundary diffusion phenomenon is possible. The strong correlation between the fraction of the equilibration attributed to each of  $\text{Fe}_{\text{Mg}}^\bullet$  and  $V_{\text{Mg}}''$  and the inferred concentration of these defects suggests that there is association between the defects. Such an association has been suggested by Tsai and Dieckmann (1997), who furthermore suggest that these neutral associates have a different concentration near grain boundaries and that the minority defect controls the rate-limiting step during re-equilibration.

Our work suggests a number of avenues for pursuit. Now that it is clear that diffusivity is  $f_{\text{O}_2}$ -dependent, we need to avoid large steps between  $f_{\text{O}_2}$  values. Diluting the experimental gas with argon will verify that a rate-limiting surface reaction is not responsible for our observations.

**Acknowledgements** This research was conducted under the financial support of IGPP-LLNL 94-12 and 95-18, and with support provided by the Office of Basic Energy Sciences of the Department of Energy under contract W7408-ENG48. Discussions and collaborations over the past few years with L. Hirsch, J. Roberts,

T. Shankland, and B.J. Wanamaker have undoubtedly influenced and enhanced our work. We would particularly like to thank S. Mackwell for advice concerning magnesium vacancy diffusivity measurements. Comments by two anonymous reviewers markedly improved the manuscript, and we would like to thank the patience of the editor while we implemented the revisions.

---

## References

- Abramowitz M, Stegun IA (1964) Handbook of mathematical functions. Dover Press, New York
- Constable SC, Duba A (1990) The electrical conductivity of olivine, a dunite, and the mantle. *J Geophys Res* 95:6967–6978
- Constable S, Roberts JJ (1997) Simultaneous modeling of thermopower and electrical conduction in olivine. *Phys Chem Miner* 24:319–325
- Crank J (1975) The mathematics of diffusion. Oxford University Press, Oxford
- Deines P, Nafziger RH, Ulmer GC, Woermann E (1974) Temperature-oxygen fugacity tables for selected gas mixtures in the system C–H–O at 1 atm total pressure. Bulletin Earth Miner Sci Exp Stn Pennsylvania State University, University Park
- Duba A, Constable SC (1993) The electrical conductivity of a lherzolite. *J Geophys Res* 98:11885–11900
- Duba A, Boland JN, Ringwood AE (1973) Electrical conductivity of pyroxene. *J Geol* 81:727–735
- Duba AG, Schock RN, Arnold E, Shankland TJ (1990) An apparatus for measurement of electrical conductivity to 1500 °C at known oxygen fugacity. In: Duba AG, Durham WB, Handin JW, Wang HF (eds) The brittle-ductile transitions in rocks. The Heard volume. *Geophys Monogr Ser*, vol. 56: AGU, Washington, DC pp. 207–210
- Franke P, Dieckmann R (1987) Point-defect relaxation in manganosite ( $Mn_{1-\Delta}$ ) after sudden oxygen activity changes in CO/CO<sub>2</sub> gas mixtures at high temperatures. In: Catlow CRA, Mackrodt WC (eds) *Advances in Ceramics*, vol. 23. Nonstoichiometric compounds. Am Ceramic Soc Westerville Ohio, pp 27–43
- Hirsch LM, Shankland TJ (1993) Quantitative olivine-defect chemical model: insights on electrical conduction, diffusion, and the role of Fe content. *Geophys J Int* 114:21–35
- Irving AJ (1980) Petrology and geochemistry of composite ultramafic xenoliths in alkalic basalts and implications for magmatic processes in the mantle. *Am J Sci* 280:389–426
- Keller M, Dieckmann R (1985) Defect structure and transport-properties of manganese oxide. I. The nonstoichiometry of manganosite ( $Mn_{1-\Delta}O$ ). *Ber Bunsen Phys Chem* 89: 883–893
- Kitazawa K, Coble RL (1974) Chemical diffusion in polycrystalline Al<sub>2</sub>O<sub>3</sub> as determined from electrical conductivity measurements. *J Am Ceramic Soc* 57:250–253
- Mackwell SJ, Dimos D, Kohlstedt DL (1988) Transient creep of olivine: point-defect relaxation times. *Philos Mag (A)* 57:779–789
- Marquardt DW (1963) An algorithm for least-squares estimation of non-linear parameters. *J Soc Ind Appl Math* 11:431–441
- Nakamura A, Schmalzried H (1984) On the Fe<sup>2+</sup>–Mg<sup>2+</sup> interdiffusion in olivine (II). *Ber Bunsenges Phys Chem* 88:140–145
- Robert JJ, Duba AG (1995) Transient electrical response of San Quintin dunite as a function of oxygen fugacity changes: information about charge carriers. *Geophys Res Lett* 22:453–456
- Schock RN, Duba A, Shankland TJ (1989) Electrical conduction in olivine. *J Geophys Res* 94:5829–5839
- Smyth DM, Stocker RL (1975) Point defects and non-stoichiometry in forsterite. *Phys Earth Planet Inter* 10:183–192
- Tsai T-L, Dieckmann R (1997) Point defects and transport of matter and charge in olivines, (Fe<sub>x</sub>Mg<sub>1-x</sub>)<sub>2</sub>SiO<sub>4</sub>. *Mat Sci Forum* Vols 239–241:399–402
- Tuller HL, Norwick AS (1977) Small polaron electron transport in reduced CeO<sub>2</sub> single crystals. *J Phys Chem Solids* 38:859–867
- Wanamaker BJ (1986) The kinetics of crack healing and the chemical and mechanical reequilibrium of fluid inclusions in San Carlos olivine. PhD Thesis, Princeton University
- Wanamaker BJ (1994) Point defect diffusivities in San Carlos olivine derived from reequilibration of electrical conductivity following changes in oxygen fugacity. *Geophys Res Lett* 21:21–24
- Wanamaker BJ, Duba AG (1993) Electrical conductivity of San Carlos olivine along (100) under oxygen- and pyroxene-buffered conditions and implications for defect equilibria. *J Geophys Res* 98:489–500